PERGAMON

International Journal of Solids and Structures 39 (2002) 765–781

INTERNATIONAL JOURNAL OF SOLIDS and STRUCTURES

www.elsevier.com/locate/ijsolstr

Nonlinear bending response and buckling of ring-stiffened cylindrical shells under pure bending

Long-yuan Li *, Roger Kettle

School of Engineering and Applied Science, Aston University, Aston Triangle, Birmingham B4 7ET, UK

Received 8 October 1999

Abstract

In this paper, the nonlinear bending response of finite length cylindrical shells with stiffening rings is investigated by using a modified Brazier approach. The basic assumptions for the present study are that the deformation of a shell subjected to pure bending can be simplified into a two-stage process. One is that the shell ovalizes but its axis remains straight; the other is that the bending of the shell is regarded as a beam with nonuniform ovalization. The nonlinear bending response is derived by applying the minimum potential energy principle and the corresponding critical moment, associated with local buckling, is determined by employing the Seide–Weingarten approximation. Numerical results are shown and compared with those obtained from other methods, which demonstrates that the assumptions used in the present study are reasonable. © 2002 Published by Elsevier Science Ltd.

Keywords: Pure bending; Buckling; Ring-stiffened cylindrical shell; Nonlinearity

1. Introduction

It is well known that when a thin-walled circular cylindrical shell is subjected to bending, its cross-section becomes progressively more oval as the curvature increases. The growth of the ovalization causes a progressive reduction in the flexural stiffness of the shell and, eventually, a maximum value of the moment is reached. Further bending occurs with a reducing moment that characterizes a limit load instability. This instability phenomenon was first investigated by Brazier (1927). He showed that when an initially straight tube is bent uniformly, the longitudinal tension and compression that resist the applied bending moment also tend to flatten or ovalize the cross-section of the tube. This in turn reduces the flexural stiffness of the member as the curvature increases. Furthermore Brazier showed that, under steadily increasing curvature, the bending moment being the product of curvature and flexural stiffness has a maximum value that is thus defined as the instability critical moment.

Brazier's simple theory was developed for cylindrical shells of infinite length. The reliability of the approach has been demonstrated by Reissner (1959) and Fabian (1977) who used robust nonlinear shell

* Corresponding author. Tel.: +44-121-3593611; fax: +44-121-3333389.
E-mail address: l.y.li@aston.ac.uk (L.-y. Li).

0020-7683/02/$ - see front matter © 2002 Published by Elsevier Science Ltd.
PII: S0020-7683(01)00174-3

equations and showed that the bending response obtained from Brazier's simple theory agrees remarkably well with the nonlinear solution. The application of Brazier's approach to finite length shells was first given by Aksel'rad (1965), who employed Valasov's semi-membrane constitutive theory to determine the effect of the cross-sectional deformation on the buckling behaviour of shells. Similar work has been done by Aksel'rad and Emmerling (1984) and Libai and Bert (1994). Tatting et al. (1995) showed that for finite length shells local buckling almost always occurs before the limit moment is reached. By employing the semi-membrane constitutive theory and Seide–Weingarten approximation (1961), Tatting et al. (1997) investigated the local buckling behaviour of composite shells exhibiting cross-sectional deformations associated with Brazier's flattening effect.

In this paper, a modified Brazier approach is used to investigate the nonlinear bending response of finite length cylindrical shells with stiffening rings. The basic assumptions used in this study are that the deformation of the shell subjected to pure bending can be simplified into a two-stage process. One is that the shell ovalizes but its axis remains straight; the other is that the bending of the shell is regarded as a beam with nonuniform ovalization. The nonlinear bending response is derived by applying the minimum potential energy principle and the corresponding critical moment associated with local buckling is determined by employing the Seide–Weingarten approximation.

2. Physical model and formulations

When a long thin-walled cylindrical shell is subjected to a static pure bending moment, the tensile and compressive longitudinal stresses on opposite sides of the neutral plane combine with the curvature of the axis of the shell to flatten its cross-section into an oval shape. Thus the deformations of the shell can be characterized by the longitudinal bending deformation (beam-type curvature) and the cross-section bending deformation (ovalization). By assuming a uniform ovalization along the length of the shell, Brazier (1927) was able to derive a simple expression for the applied moment as a function of the longitudinal bending curvature. However, for shells of finite length, or with stiffening rings, the ovalization of the cross-section is no longer uniform because of the local effects of the boundaries or stiffening rings. In order to extend Brazier's approach to a general case, the following displacements are assumed for the shell subjected to a static pure bending moment:

$$u(x,\theta) = u_1(x)\cos\theta + u_2(x)\cos 2\theta \tag{1a}$$

$$v(x,\theta) = v_1(x)\sin\theta + v_2(x)\sin 2\theta \tag{1b}$$

$$w(x,\theta) = w_1(x)\cos\theta + w_2(x)\cos 2\theta \tag{1c}$$

where $u(x,\theta)$, $v(x,\theta)$ and $w(x,\theta)$ are the axial, circumferential, and radial displacements of the point (x,θ) on the shell middle surface, θ is the angular coordinate measured from the vertical axis as shown in Fig. 1.

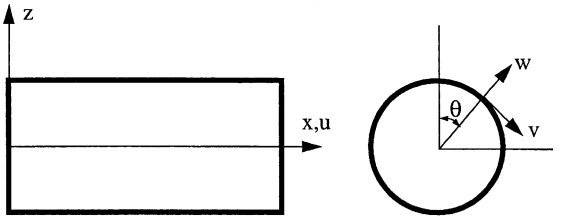

Fig. 1. Shell geometry and coordinate system used.

The displacement components $u_1(x)$, $v_1(x)$ and $w_1(x)$ represent the overall longitudinal bending deformation of the shell which behaviours like a beam, whereas $u_2(x)$, $v_2(x)$ and $w_2(x)$ are the displacements related to the ovalization deformation. The membrane and bending strains of the shell are obtained in terms of these displacements and their derivatives by:

$$\varepsilon_x = \frac{\partial u}{\partial x} \tag{2a}$$

$$\varepsilon_\theta = \frac{1}{R}\left(\frac{\partial v}{\partial \theta} + w\right) \tag{2b}$$

$$\gamma_{x\theta} = \frac{1}{R}\frac{\partial u}{\partial \theta} + \frac{\partial v}{\partial x} \tag{2c}$$

$$\kappa_x = \frac{\partial^2 w}{\partial x^2} \tag{2d}$$

$$\kappa_\theta = -\frac{1}{R^2}\left(\frac{\partial^2 w}{\partial \theta^2} - \frac{\partial v}{\partial \theta}\right) \tag{2e}$$

$$\kappa_{x\theta} = -\frac{1}{R}\left(\frac{\partial^2 w}{\partial \theta \partial x} - \frac{\partial v}{\partial x}\right) \tag{2f}$$

where ε_x, ε_θ and $\gamma_{x\theta}$ are the membrane strains, κ_x, κ_θ and $\kappa_{x\theta}$ are the bending strains, and R is the mean radius of the shell.

In order to simplify the problem, we first utilize Brazier's condition for the inextensionality of the cross-section. This implies that the circumferential membrane strain ε_θ is zero. Substituting Eqs. (1b) and (1c) into Eq. (2b) yields,

$$\varepsilon_\theta = \frac{1}{R}[(v_1 + w_1)\cos\theta + (2v_2 + w_2)\cos 2\theta] = 0 \tag{3}$$

Therefore, we have,

$$v_1 = -w_1 \quad \text{and} \quad v_2 = -\frac{w_2}{2} \tag{4}$$

We next utilize the assumptions of Vlasov's semi-membrane constitutive theory (Vasiliev, 1993), in which the shell is assumed to have no rigidities in axial bending and twisting. We then have,

$$M_x = 0 \quad \text{and} \quad M_{x\theta} = 0 \tag{5}$$

where M_x and $M_{x\theta}$ are the axial bending and twisting moments, respectively. The above semi-membrane constitutive theory assumptions were also used by Aksel'rad and Emmerling (1984), Libai and Bert (1994) and Tatting et al. (1997) for the problem of pure bending of finite length shells.

With these assumptions only the axial membrane and shear strains, and the circumferential bending strain need to be considered. Substituting Eqs. (1a)–(1c) into Eqs. (2a), (2c) and (2e) and using Eq. (4), we have,

$$\varepsilon_x = \frac{\mathrm{d}u_1}{\mathrm{d}x}\cos\theta + \frac{\mathrm{d}u_2}{\mathrm{d}x}\cos 2\theta \tag{6a}$$

$$\gamma_{x\theta} = -\left(\frac{u_1}{R} + \frac{\mathrm{d}w_1}{\mathrm{d}x}\right)\sin\theta - \left(\frac{2u_2}{R} + \frac{1}{2}\frac{\mathrm{d}w_2}{\mathrm{d}x}\right)\sin 2\theta \tag{6b}$$

$$\kappa_\theta = \frac{3w_2}{R^2}\cos 2\theta \tag{6c}$$

Note that the first term of the shear strain corresponding to $\sin\theta$ should be zero since the overall bending of the shell as a beam does not generate shear strain in the case of pure bending. Thus, we have

$$\frac{u_1}{R} = -\frac{\mathrm{d}w_1}{\mathrm{d}x} \tag{7}$$

Substituting Eq. (7) into Eqs. (6a) and (6b) yields,

$$\varepsilon_x = -R\frac{\mathrm{d}^2 w_1}{\mathrm{d}x^2}\cos\theta + \frac{\mathrm{d}u_2}{\mathrm{d}x}\cos 2\theta \tag{8a}$$

$$\gamma_{x\theta} = -\left(\frac{2u_2}{R} + \frac{1}{2}\frac{\mathrm{d}w_2}{\mathrm{d}x}\right)\sin 2\theta \tag{8b}$$

The total strain energy of the stiffened shell can be calculated by assuming the deformation of the shell as a two-stage process. In the first stage the shell ovalizes in a way which is compatible with the assumed ovalization deformation but its axis remains straight; and in the second stage the shell bends as a beam with nonuniform cross-section, subjected to a constant bending moment. This assumption of a two-stage deformation process was first made by Brazier (1927) in his early work for infinite length shells and lately extended by Calladine (1983) to finite length shells.

The strain energies involved in the first stage are those associated with the axial membrane and shear strains of the shell, and the circumferential bending strains of the shell and stiffening rings, which can be expressed by:

$$U_1 = \frac{h}{2}\int_0^L\int_0^{2\pi}\left(E_x\varepsilon_{x2}^2 + G_{x\theta}\gamma_{x\theta}^2\right)\mathrm{d}x R\,\mathrm{d}\theta + \frac{D_\theta}{2}\int_0^L\int_0^{2\pi}\kappa_\theta^2\,\mathrm{d}x R\,\mathrm{d}\theta + \sum_{n=1}^{N}\frac{EI_{\mathrm{ring}}}{2}\int_0^{2\pi}\kappa_\theta^2 R\,\mathrm{d}\theta \tag{9}$$

where h is the thickness of the shell, L is the length of the shell, E_x is the elastic modulus of the shell in the axial direction, $G_{x\theta}$ is the shear modulus of the shell, D_θ is the bending rigidity of the shell in the circumferential direction, EI_{ring} is the bending rigidity of the stiffening ring, N is the total number of stiffeners, and ε_{x2} is the part of the axial membrane strain corresponding to $\cos 2\theta$. Here the stiffening ringers have been assumed to be evenly spaced and symmetric with respect to the shell middle surface. Substituting Eqs. (6c), (8a) and (8b) into Eq. (9) yields,

$$\begin{aligned} U_1 = {} & \frac{\pi hR}{2}\int_0^L\left[E_x\left(\frac{\mathrm{d}u_2}{\mathrm{d}x}\right)^2 + G_{x\theta}\left(\frac{2u_2}{R} + \frac{1}{2}\frac{\mathrm{d}w_2}{\mathrm{d}x}\right)^2\right]\mathrm{d}x + \frac{\pi RD_\theta}{2}\int_0^L\left(\frac{3w_2}{R^2}\right)^2\mathrm{d}x \\ & + \sum_{n=1}^{N}\frac{\pi REI_{\mathrm{ring}}}{2}\left(\frac{3w_2(x)}{R^2}\bigg|_{x=x_n}\right)^2 \end{aligned} \tag{10}$$

where x_n is the position where a stiffener is placed. In the second stage the strain energy is only related to the axial membrane strain corresponding to $\cos\theta$:

$$U_2 = \frac{E_x h}{2}\int_0^L\int_0^{2\pi R}\varepsilon_{x1}^2\,\mathrm{d}x\,\mathrm{d}s \approx \frac{E_x h}{2}\int_0^L\int_0^{2\pi R}\left(\frac{\mathrm{d}^2 w_1}{\mathrm{d}x^2}z\right)^2\mathrm{d}x\,\mathrm{d}s \tag{11}$$

where ε_{x1} is the part of the axial membrane strain corresponding to $\cos\theta$. Note that the first integration in Eq. (11) is based on the undeformed shell, while the second one is on the deformed shell in which the axial strain is assumed to be linear with the distance from the neutral axis and proportional to the longitudinal bending curvature of the axis of the shell. This energy can also be rewritten into the longitudinal bending strain energy of the shell as a beam:

$$U_2 = \frac{1}{2}\int_0^L E_x I_{\text{shell}} C^2 \,\mathrm{d}x \tag{12}$$

where $E_x I_{\text{shell}}$ is the bending rigidity of the shell as a beam and C is the longitudinal bending curvature of the axis of the shell. Taking into account the effects of the ovalization, I_{shell} has an expression:

$$I_{\text{shell}} = Rh\int_0^{2\pi} [(R + w_2\cos 2\theta)\cos\theta - (v_2 \sin 2\theta)\sin\theta]^2 \,\mathrm{d}\theta \approx \pi R^3 h\left(1 + \frac{3}{2}\frac{w_2}{R}\right) \tag{13}$$

The longitudinal bending curvature of the axis of the shell can be obtained in terms of the displacement $v_1(x)$ or $w_1(x)$ as follows:

$$C = -\left.\frac{\partial^2 v}{\partial x^2}\right|_{\theta=\frac{\pi}{2}} = -\frac{\mathrm{d}^2 v_1}{\mathrm{d}x^2} = \frac{\mathrm{d}^2 w_1}{\mathrm{d}x^2} \tag{14}$$

Substituting Eqs. (13) and (14) into Eq. (12) yields,

$$U_2 = \frac{\pi R^3 h E_x}{2}\int_0^L \left(1 + \frac{3}{2}\frac{w_2}{R}\right)\left(\frac{\mathrm{d}^2 w_1}{\mathrm{d}x^2}\right)^2 \mathrm{d}x \tag{15}$$

The potential of the applied moments is expressed by:

$$W = 2M\Omega = M\int_0^L \left(\frac{\mathrm{d}^2 w_1}{\mathrm{d}x^2}\right)\mathrm{d}x = M\left[\left.\frac{\mathrm{d}w_1}{\mathrm{d}x}\right|_{x=L} - \left.\frac{\mathrm{d}w_1}{\mathrm{d}x}\right|_{x=0}\right] \tag{16}$$

where M is the applied moment and Ω is the end rotation. The total potential of the system is expressed by:

$$\Pi\left(u_2, \frac{\mathrm{d}w_1}{\mathrm{d}x}, w_2\right) = U_1 + U_2 - W \tag{17}$$

from which the nonlinear bending response of the stiffened shell under pure bending can be derived.

3. Nonlinear bending responses of stiffened shells subjected to pure bending

Consider the shell with the boundary conditions of simply supported for $w(x,\theta)$ ($w(x,\theta) = 0$ at $x = 0$ and L), cross-sectional shape restraint for $v(x,\theta)$ ($v(x,\theta) = 0$ at $x = 0$ and L) and rigid rotated ends for $u(x,\theta)$ ($u(x,\theta) = \Omega R\cos\theta$ at $x = 0$ and L). If we expand the displacements in terms of a Fourier series in the axial direction as follows:

$$\frac{u_1(x)}{R} = -\frac{\mathrm{d}}{\mathrm{d}x}w_1(x) = \left(\frac{R}{L}\right)\left[\xi_0\left(1 - \frac{2x}{L}\right) - \sum_{k=2,4}^{\infty}\frac{\xi_k}{k\pi}\sin\frac{k\pi x}{L}\right] \tag{18a}$$

$$\frac{u_2(x)}{R} = \sum_{m=2,4}^{\infty}\left(\frac{R}{L}\right)\eta_m \sin\frac{m\pi x}{L} \tag{18b}$$

$$\frac{w_2(x)}{R} = -\sum_{n=1,3}^{\infty} \zeta_n \sin\frac{n\pi x}{L} \tag{18c}$$

where ξ_0, ξ_k, η_m, ζ_n are constants to be determined, the above boundary conditions are satisfied. Substituting Eqs. (18a)–(18c) into Eqs. (10), (15) and (16) yields,

$$\frac{U_1}{A} = \sum_{m=2}^{\infty}(m\pi\eta_m)^2 + \mu^2\left[\sum_{m=2}^{\infty}(2\eta_m)^2 + \sum_{n=1}^{\infty}\left(\frac{n\pi\zeta_n}{2}\right)^2\right] - 8\mu^2\left[\sum_{m=2}^{\infty}\sum_{n=1}^{\infty}\frac{mn\eta_m\zeta_n}{m^2-n^2}\right] + 4\lambda^4(1+\beta) \times \sum_{n=1}^{\infty}\zeta_n^2 - 4\lambda^4\beta\sum_{n=1}^{\infty}\zeta_n\zeta_{2(N+1)-n} \tag{19a}$$

$$\frac{U_2}{A} = 8\xi_0^2 - \frac{24}{\pi}\xi_0^2\sum_{n=1}^{\infty}\frac{\zeta_n}{n} - \frac{24}{\pi}\xi_0\sum_{k=2}^{\infty}\sum_{n=1}^{\infty}\frac{n\xi_k\zeta_n}{n^2-k^2} + \sum_{k=2}^{\infty}\xi_k^2 - \frac{3}{\pi}\sum_{k=2}^{\infty}\sum_{k'=2}^{\infty}\sum_{n=1}^{\infty}\left(\frac{n\xi_k\xi_{k'}\zeta_n}{n^2-(k+k')^2} + \frac{n\xi_k\xi_{k'}\zeta_n}{n^2-(k-k')^2}\right) \tag{19b}$$

$$\frac{W}{A} = 16\Lambda\xi_0 \tag{19c}$$

in which,

$$A = \frac{\pi R^5 h E_x}{4L^3} = \text{an energy factor} \tag{20a}$$

$$\beta = \frac{(N+1)EI_{\text{ring}}}{D_\theta L} = \text{the bending rigidity parameter of stiffeners} \tag{20b}$$

$$\mu = \sqrt{\frac{L^2 G_{x\theta}}{R^2 E_x}} = \text{the shear length parameter} \tag{20c}$$

$$\lambda = \sqrt[4]{\frac{9L^4 D_\theta}{4hR^6 E_x}} = \text{the shell length parameter} \tag{20d}$$

$$\Lambda = \frac{ML^2}{2\pi R^4 h E_x} = \text{the applied moment parameter} \tag{20e}$$

In the derivation of Eq. (19a) the stiffening rings have been assumed to be uniformly distributed over the shell length, each of which has the same bending rigidity. Applying the following minimum potential energy principle:

$$\frac{\partial\Pi}{\partial\xi_k} = 0 \quad k = 0, 2, 4, \ldots \tag{21a}$$

$$\frac{\partial \Pi}{\partial \eta_m} = 0 \quad m = 2,4,6,\ldots \tag{21b}$$

$$\frac{\partial \Pi}{\partial \zeta_n} = 0 \quad n = 1,3,5,\ldots \tag{21c}$$

we have,

$$\xi_0 - \frac{3}{\pi}\xi_0 \sum_{n=1}^{\infty} \frac{\zeta_n}{n} - \frac{3}{2\pi} \sum_{k=2}^{\infty} \sum_{n=1}^{\infty} \frac{n\xi_k \zeta_n}{n^2 - k^2} = \Lambda \tag{22a}$$

$$\xi_k - \frac{12}{\pi}\xi_0 \sum_{n=1}^{\infty} \frac{n\zeta_n}{n^2 - k^2} - \frac{3}{\pi} \sum_{k'=2}^{\infty} \sum_{n=1}^{\infty} \left(\frac{n\xi_{k'}\zeta_n}{n^2 - (k+k')^2} + \frac{n\xi_{k'}\zeta_n}{n^2 - (k-k')^2} \right) = 0 \quad k = 2,4,\ldots \tag{22b}$$

$$\left[1 + \left(\frac{m\pi}{2\mu} \right)^2 \right] \eta_m - \sum_{n=1}^{\infty} \frac{mn\zeta_n}{m^2 - n^2} = 0 \quad m = 2,4,\ldots \tag{22c}$$

$$\left[\left(\frac{n\pi}{4} \right)^2 + \left(\frac{\lambda^2}{\mu} \right)^2 (1+\beta) \right] \zeta_n - \left(\frac{\lambda^2}{\mu} \right)^2 \beta \zeta_{2(N+1)-n} - \sum_{m=2}^{\infty} \frac{mn\eta_m}{m^2 - n^2} - \frac{3}{\pi\mu^2} \frac{\xi_0^2}{n} - \frac{3}{\pi\mu^2} \xi_0 \sum_{k=2}^{\infty} \frac{n\xi_k}{n^2 - k^2}$$
$$- \frac{3}{8\pi\mu^2} \sum_{k'=2}^{\infty} \sum_{k=2}^{\infty} \left(\frac{n\xi_{k'}\xi_k}{n^2 - (k+k')^2} + \frac{n\xi_{k'}\xi_k}{n^2 - (k-k')^2} \right) = 0 \quad n = 1,3,\ldots$$

The examination of the order of magnitude of the variables ξ_0, ξ_k, η_m, ζ_n shows that variables ξ_k, η_m, ζ_n are one order of magnitude smaller than the variable ξ_0. This is due to the fact that for the shell subjected to a pure bending the dominant deformation is the bending deformation. By neglecting the nonlinear terms of the low order variables, Eqs. (22a)–(22d) can be simplified as:

$$\xi_0 - \frac{3}{\pi}\xi_0 \sum_{n=1}^{\infty} \left(\frac{\zeta_n}{n} \right) = \Lambda \tag{23a}$$

$$\xi_k = \frac{12}{\pi}\xi_0 \sum_{n=1}^{\infty} \frac{n^2}{n^2 - k^2} \left(\frac{\zeta_n}{n} \right) \quad k = 2,4,\ldots \tag{23b}$$

$$\left(\frac{\eta_m}{m} \right) = \frac{(2\mu)^2}{(2\mu)^2 + (m\pi)^2} \sum_{n=1}^{\infty} \frac{n^2}{m^2 - n^2} \left(\frac{\zeta_n}{n} \right) \quad m = 2,4,\ldots \tag{23c}$$

$$\left[\left(\frac{n\pi}{4} \right)^2 + (1+\beta) \left(\frac{\lambda^2}{\mu} \right)^2 \right] \left(\frac{\zeta_n}{n} \right) - \beta \left(\frac{\lambda^2}{\mu} \right)^2 \left(\frac{2(N+1)-n}{n} \right) \left(\frac{\zeta 2(N+1)-n}{2(N+1)-n} \right)$$
$$\left(- \sum_{m=2}^{\infty} \frac{m^2}{m^2 - n^2} \left(\frac{\eta_m}{m} \right) \right) - \frac{3}{\pi\mu^2} \left(\frac{\xi_0}{n} \right)^2 - \frac{3}{\pi\mu^2} \xi_0 \sum_{k=2}^{\infty} \frac{\xi_k}{n^2 - k^2} = 0 \quad n = 1,3,\ldots \tag{23d}$$

Substituting Eqs. (23b) and (23c) into Eq. (23d) and noting that $\xi_0 = \Omega(L/R)$, Eqs. (23a) and (23d) become:

$$\left(\frac{\Lambda}{\mu} \right) = \left(\frac{L\Omega}{R\mu} \right) \left[1 - \frac{3}{\pi} \sum_{n=1}^{\infty} \left(\frac{\zeta_n}{n} \right) \right] \tag{24a}$$

$$\left[\left(\frac{n\pi}{4}\right)^2+(1+\beta)\left(\frac{\lambda^2}{\mu}\right)^2\right]\left(\frac{\zeta_n}{n}\right)-\beta\left(\frac{\lambda^2}{\mu}\right)^2\left(\frac{2(N+1)-n}{n}\right)\left(\frac{\zeta 2(N+1)-n}{2(N+1)-n}\right)$$
$$+\sum_{j=1}^{\infty}F_1(j,n,\mu)\left(\frac{\zeta_j}{j}\right)-\left(\frac{6}{\pi}\right)^2\left(\frac{L\Omega}{R\mu}\right)^2\sum_{j=1}^{\infty}F_2(j,n)\left(\frac{\zeta_j}{j}\right)=\frac{3}{\pi}\frac{1}{n^2}\left(\frac{L\Omega}{R\mu}\right)^2 \quad n=1,3,5,\ldots \tag{24b}$$

in which,

$$F_1(j,n,\mu)=\sum_{m=2}^{\infty}\frac{m^2}{m^2-n^2}\frac{j^2}{j^2-m^2}\frac{(2\mu)^2}{(2\mu)^2+(m\pi)^2} \tag{25a}$$

$$F_2(j,n)=\sum_{k=2}^{\infty}\frac{1}{n^2-k^2}\frac{j^2}{j^2-k^2} \tag{25b}$$

Note that the set of Eq. (24b) is linear about the variable ζ_n if the end rotation Ω is regarded as a known. Thus, for a given end rotation, we can solve Eq. (24b) to find the ovalization variable ζ_n for various values of n and then calculate Λ directly from Eq. (24a). In this way, we do not need to solve any nonlinear equation.

For smooth shells of infinite length ($\lambda\to\infty$, $\beta=0$), Eq. (24b) becomes,

$$\lambda^4\left(\frac{\zeta_n}{n}\right)=\frac{1}{n^2}\frac{3}{\pi}\left(\frac{L\Omega}{R}\right)^2 \tag{26}$$

Substituting Eq. (26) into Eq. (25a) yields,

$$\left(\frac{L\Omega}{R}\right)\left[1-\frac{9}{8}\left(\frac{L\Omega}{R}\right)^2\frac{1}{\lambda^4}\right]=\Lambda \tag{27}$$

From this nonlinear moment–end rotation relationship the following maximum moment is obtained:

$$\Lambda_{\max}=\frac{4\sqrt{2}}{9\sqrt{3}}\lambda^2 \tag{28a}$$

or

$$\frac{M_{\max}}{M_0}=\left(\frac{4\sqrt{2}}{3\sqrt{3}}\right)\sqrt{\frac{D_\theta E_x}{D_{11}E_\theta}}=0.544\sqrt{\frac{D_\theta E_x}{D_{11}E_\theta}} \tag{28b}$$

where $M_0=2\pi R\sqrt{D_{11}E_\theta}h$ is the classical buckling critical moment, D_{11} is the bending rigidity of the shell in the axial direction and E_θ is the elastic modulus of the shell in the circumferential direction. The limit instability moment given by Eq. (28b) is the well-known Brazier's critical moment for long orthotropic tubes (Li, 1996). For an isotropic shell this limit instability moment is only about 0.544 times the classical buckling critical moment.

4. Determination of critical moment due to local buckling

The nonlinear bending response (moment versus end rotation) determined by Eqs. (24a) and (24b) has a maximum value for the moment. This maximum moment defines the limit instability moment of finite length shells with stiffening rings. For a member subjected to a compressive stress, however, bifurcation instability may also occur. Many investigators have found that for shells of finite length subjected to pure

bending the local bifurcation buckling almost always occurs before the limit moment is reached (Tatting et al., 1995; Stephens et al., 1975). Indeed, as is shown in the Appendix A, even for isotropic shells of infinite length this conclusion still holds.

The bifurcation buckling of circular cylindrical shells of intermediate length under bending can be determined using the approach suggested by Seide and Weingarten (1961). For orthotropic shells, this critical stress is expressed by (Tatting et al., 1997):

$$\sigma_{\mathrm{cr}} = \frac{-2\sqrt{D_{11}E_\theta h}}{\rho h} \tag{29}$$

where ρ is the local radius of circumferential curvature of the cylinder at $\theta = 0$. As it has been shown, "due to the Brazier effect, the cross-section of the cylinder deforms into an oval and the radius of curvature at the critical location increases, thus lowering the critical buckling stress" (Tatting et al., 1997). Therefore, the collapse moment can be determined by examining when the axial stress on the compressive side of the cylinder reaches this critical value. The maximum axially compressive stress can be calculated either by:

$$\sigma_x = -E_x\varepsilon_x|_{\theta=0} = -E_x\left(\frac{\mathrm{d}u_1}{\mathrm{d}x} + \frac{\mathrm{d}u_2}{\mathrm{d}x}\right) \tag{30a}$$

or simply in terms of the stress formula of the beam in bending

$$\sigma_x = -\frac{M}{I_{\mathrm{shell}}}(R + w_2) \tag{30b}$$

where I_{shell} is the second moment of the cross-section of deformed shell defined by Eq. (13). The local radius of circumferential curvature can be calculated by (derivation of Eq. (31) is given in Appendix B)

$$\rho = \frac{R^2}{R + 3w_2} \tag{31}$$

5. Numerical results

The nonlinear bending responses of shells without stiffeners are first investigated and the results are shown in Fig. 2 for various values of λ when $\mu = 1$, in which the applied moment and end rotation have been normalized with respect to their classical buckling values for an infinite length cylinder, and the collapse parameter has been assumed to be equal to 1:

$$\overline{m} = \frac{M}{2\pi R\sqrt{D_{11}E_\theta h}} = \Lambda\left(\frac{R^3}{hL^2}\right)\sqrt{\frac{h^3E_x^2}{D_{11}E_\theta}} \tag{32a}$$

$$\bar{\alpha} = \left(\Omega\frac{L}{R}\right)\left(\frac{R^3}{hL^2}\right)\sqrt{\frac{h^3E_x^2}{D_{11}E_\theta}} \tag{32b}$$

$$\sqrt{\frac{D_{11}E_\theta}{D_\theta E_x}} = 1 \tag{32c}$$

It can be seen that, for very small values of the shell length parameter, λ, which correspond to short and very thin cylinders, there is almost no ovalization before buckling and thus the pre-buckling path remains linear and buckling occurs at the classical value. As λ increases, the effect of the Brazier nonlinearity becomes more important and the buckling critical moment tends closer to the Brazier's limit moment.

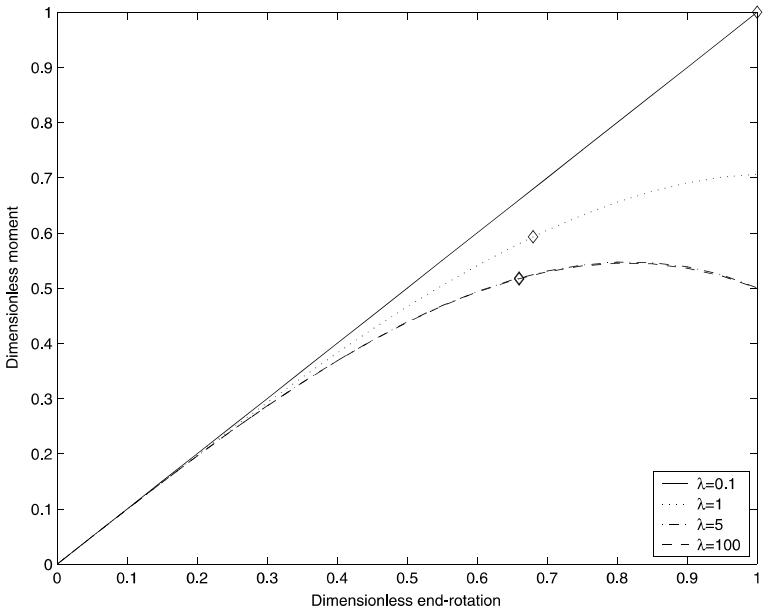

Fig. 2. Applied moment ($\bar{m}$) versus end rotation ($\bar{\alpha}$) for $\mu = 1.0$ (diamond symbol represents the bifurcation buckling point).

Fig. 3 shows the bending responses of shells for various values of μ when $\lambda = 1$. Small values of the shear length parameter, μ, imply the boundaries having little influence on the ovalization deformation. Thus, the

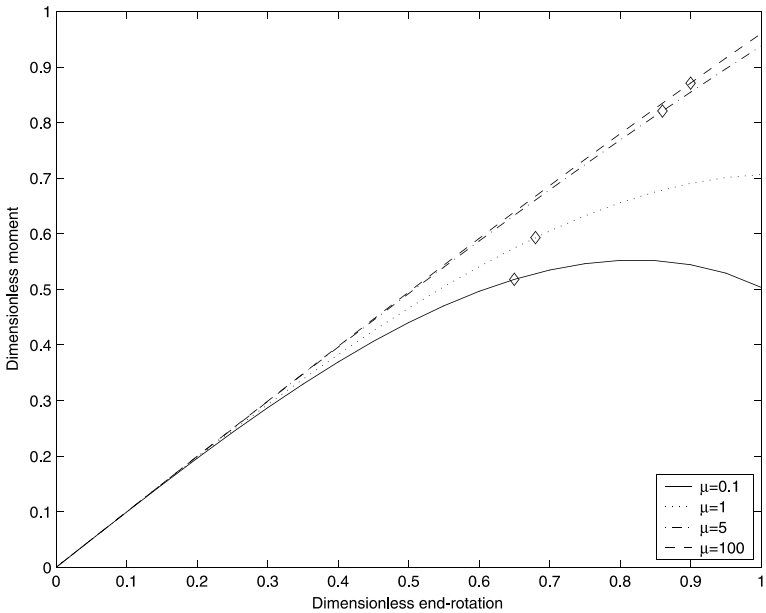

Fig. 3. Applied moment ($\bar{m}$) versus end rotation ($\bar{\alpha}$) for $\lambda = 1.0$ (diamond symbol represents the bifurcation buckling point).

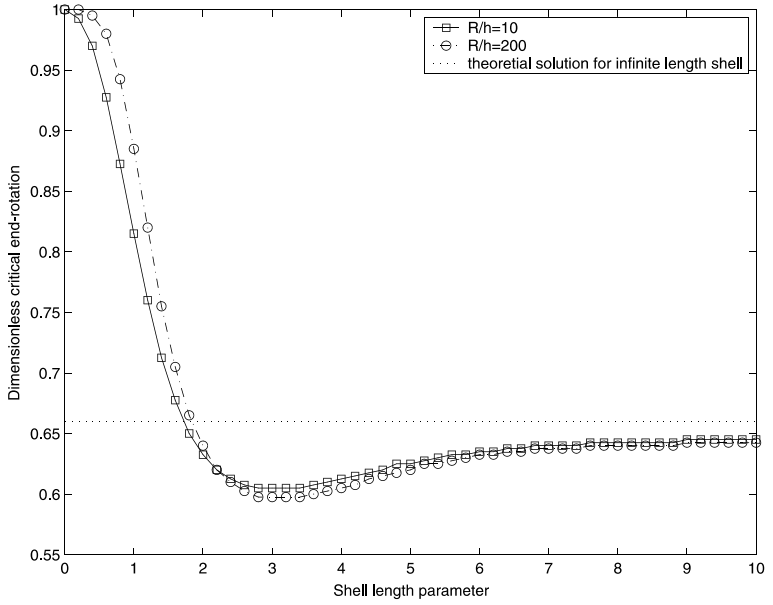

Fig. 4. Critical end rotation ($\bar{\alpha}$) versus shell length parameter (λ).

effect of the Brazier nonlinearity is important and the buckling critical moment, as to be expected, is close to the Brazier's limit moment. With the increase of the shear length parameter, the boundary influence becomes more important and thus the ovalization deformation becomes smaller. For very large value of μ, the pre-buckling path is almost linear and thus buckling critical moment is close to the classical value.

The curves of moment versus end rotation shown in Figs. 2 and 3 agree very well with those reported by Tatting et al. (1997). The critical moments obtained here are also very close to those given by Tatting et al. (1997) except for that with very large μ value (i.e., for very short cylinders) in which case the present model is not applicable.

Fig. 4 shows the variation of the critical end rotations with the shell length parameter λ for two ratios of $R/h = 10$ and $R/h = 200$, respectively. The results for those between these two ratios are not presented here because they were found very similar and to lie between the two presented curves. It is of interest to find that for $\lambda > 2$ the ratio, R/h, does not have a significant influence on the solution. With the increase of λ both solutions gradually tend to the analytical solution of infinite length shells (its derivation is given in Appendix A). The main deviation between the two solutions is found for short shells which is due to the shear influence. For a given tube length parameter λ, an increase in R/h implies an increase in the shear length parameter μ, and so a higher buckling critical moment is expected for a higher value of R/h.

The variation of the critical moments with the shell length parameter λ for $R/h = 10$ and $R/h = 200$ is shown in Fig. 5. As to be expected, the critical moment decreases with the increase of the shell length parameter. The difference of the two curves is found mainly in the region for $\lambda < 2$ where the shear deformation plays an important role. For long shells, the two curves merge together and tend to the analytical solution of infinite length shells as $\lambda \to \infty$. In order to demonstrate the reliability of the model established in this study the critical moments obtained from other methods are also given in Fig. 5. It is found that our results agree very well with those given by Libai and Bert (1994) and Tatting et al. (1997). Note that the results in Libai and Bert (1994) were obtained by ignoring the shear warping. Thus, they are only comparable with those related to small values of the shear length parameter ($R/h = 10$).

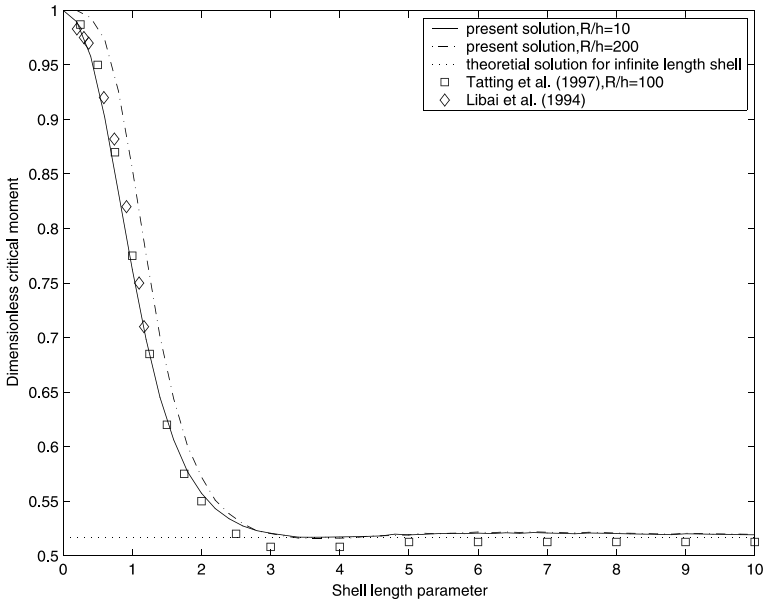

Fig. 5. Critical moment ($\bar{m}$) versus shell length parameter (λ).

It should be mentioned that the difference between the present model and that developed by Tatting et al. (1997) is the axial displacement assumed and the method used to solve the governing differential equations. Although the axial displacement employed in the present model has one less term than that used in the Tatting's model and some simplification is used in solving the nonlinear equations, the results obtained are very close to those provided by Tatting et al. (1997). This demonstrates that the assumptions made in the present model are reasonably acceptable.

The influence of the stiffening rings on the critical moment and the corresponding end rotation is shown in Fig. 6. It can be seen that the use of stiffeners can significantly increase the critical moment for long shells where the ovalization of the shell cross-section has a significant influence on the local buckling of the shell. For very short shells, the stiffeners have very little influence on the critical moment. This is because the ovalization is very small for short shells and so there is no remarkable difference between smooth and stiffened shells.

Fig. 7 shows the variation of critical moments and the corresponding end rotations with the stiffener rigidity parameter for $\lambda = 2$ and $\lambda = 10$, respectively. As expected, in both cases the critical moment and corresponding end rotation increase with the stiffener rigidity. However, the increase of critical moment and corresponding end rotation seems to be limited in the case of $\lambda = 10$ when the number of stiffeners is fixed. This is because as $\beta \to \infty$, the bending of a long stiffened shell becomes the same as that of a number of short shells, the length of which is equal to the space between the individual stiffeners.

Fig. 8 shows the influence of the number of stiffeners on the critical moment and corresponding end rotation. Note that as the number of stiffeners is increased, the rigidity of each stiffener is reduced since the bending rigidity parameter β is identical in each case. It is found that, both the critical moment and corresponding end rotation increase initially with the number of stiffeners. With the further increase, the space between the individual stiffeners is reduced so that a smear stiffener model can be applied. Therefore the stiffener number has no influence on the buckling behaviour of the shell after it reaches to a certain level.

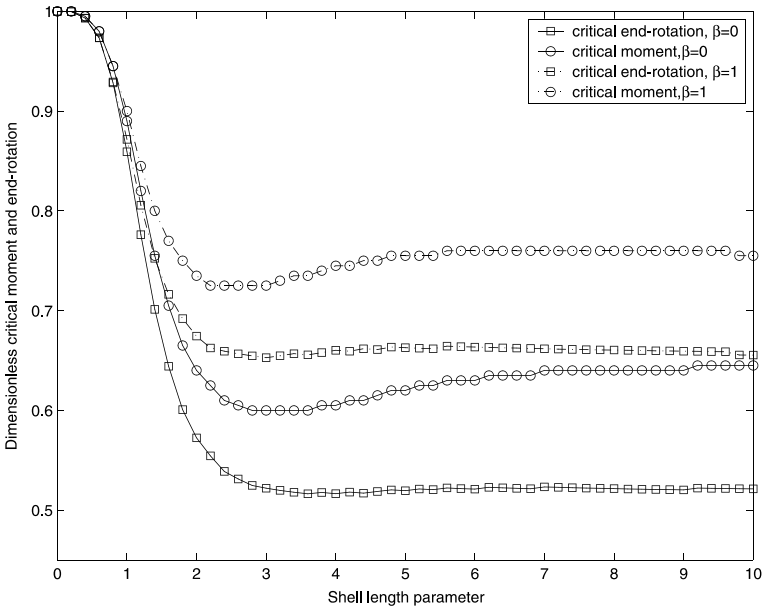

Fig. 6. Critical moment ($\bar{m}$) and end rotation ($\bar{\alpha}$) versus shell length parameter (λ) for smooth ($\beta = 0$) and stiffened shells ($\beta = 1$) ($R/h = 200$, $N = 10$).

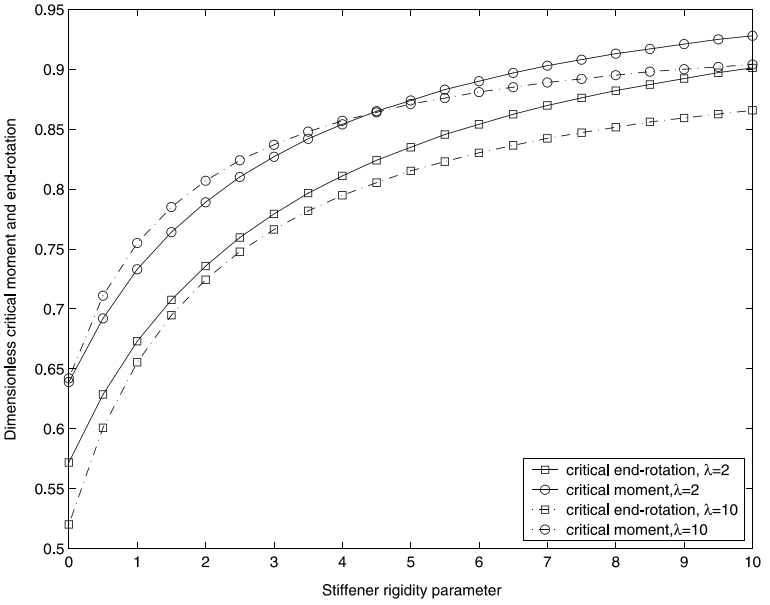

Fig. 7. Critical moment ($\bar{m}$) and end rotation ($\bar{\alpha}$) versus the stiffener rigidity parameter (β) for stiffened shells with different values of λ ($R/h = 200$, $N = 10$).

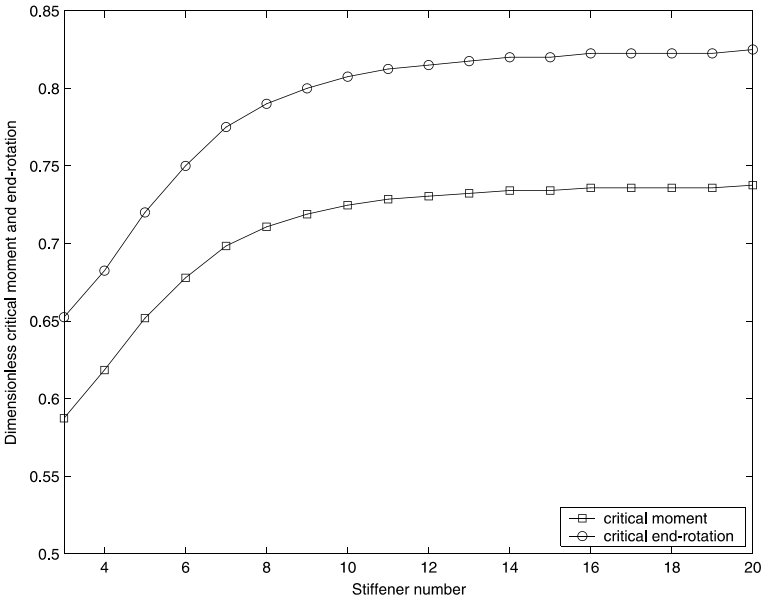

Fig. 8. Critical moment ($\bar{m}$) and end rotation ($\bar{\alpha}$) versus the stiffener number (N) for the stiffened shell ($\lambda = 10$, $R/h = 200$, $\beta = 2$).

6. Conclusions

The nonlinear bending responses of finite length shells with and without stiffening rings subjected to pure bending have been investigated. The problem has been solved by modifying the Brazier approach and employing the semi-membrane constitutive theory. The nonlinear bending response is determined in a way in which solving nonlinear equations can be avoided. The stability of the shell due to local buckling has been determined by using Seide–Weingarten approximation. The influence of Brazier nonlinearity on the critical moment has been discussed. Results have been compared with those obtained from other methods, which demonstrates that the assumptions used in the present study are suitable.

It has been shown that the critical moment increases with both the number and rigidity of stiffeners. This increase is because the stiffeners can resist the ovalization deformation and thus enhance the overall bending rigidity of the shell.

Finally, it should be mentioned that the buckling investigated in the present study is restricted to the case where the ovalization deformation is dominant and thus the results obtained from this study is applicable only to intermediate and long cylindrical shells with light stiffening rings. For shells with heavy stiffening rings the present results may be applied when the stiffener spacing is long enough in which case the ovalization deformation is still dominant.

Appendix A. Derivation of critical moment for infinite length isotropic tubes

In terms of Brazier simple approach, the moment versus end rotation relationship for an infinite length tube under pure bending can be expressed as follows (Li, 1996):

$$\frac{M}{M_b} = \frac{3}{2}\left(1 - \frac{3}{2}\xi\right)\left(\frac{C}{C_b}\right) \tag{A.1}$$

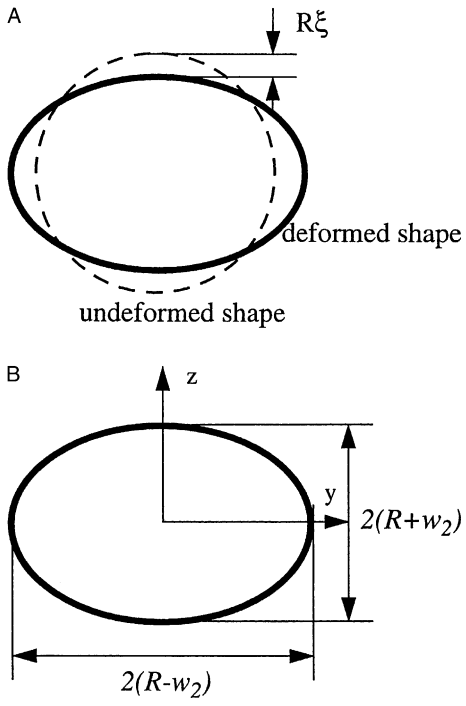

Fig. 9. (A) The deformed geometry of the shell cross-section. (B) The deformed cross-section.

$$\xi = \frac{2}{9}\left(\frac{C}{C_b}\right)^2 \tag{A.2}$$

where M is the applied moment, C is the longitudinal bending curvature of the tube axis, and ξ is the dimensionless parameter characterizing the maximum flattening in bending at the extreme fibers (see Fig. 9(A)). M_b and C_b are the Brazier's limit moment and corresponding bending curvature defined by:

$$M_b = \frac{2\sqrt{2}}{3\sqrt{3}}M_0 \quad \text{and} \quad C_b = \frac{\sqrt{2}}{\sqrt{3}}C_0 \tag{A.3}$$

$$M_0 = \frac{\pi R h^2 E}{\sqrt{3(1-\nu^2)}} = \text{the classical critical moment} \tag{A.4}$$

$$C_0 = \frac{h}{R^2\sqrt{3(1-\nu^2)}} = \text{the classical critical curvature} \tag{A.5}$$

The largest compressive stress of the tube during pure bending can be calculated by:

$$\sigma = \frac{MR}{I_{shell}}(1-\xi) \tag{A.6}$$

where I_{shell} is the second moment of the cross-section of the tube, which, considering the ovalization deformation, has the following approximate expression (see Eq. (13)):

$$I = \pi R^3 h\left(1 - \tfrac{3}{2}\xi\right) \tag{A.7}$$

Substituting Eq. (A.7) into Eq. (A.6) yields,

$$\sigma = \frac{M}{\pi R^2 h}\frac{1-\xi}{1-\frac{3}{2}\xi} \tag{A.8}$$

The largest radius of circumferential curvature of deformed tube is at the point where the compressive stress is also the largest, and can be expressed by (see Eq. (31) and $w_2 = -\xi R$)

$$\rho = \frac{R}{1-3\xi} \tag{A.9}$$

According to Seide and Weingarten (1961) approximation, for the pure bending of a long tube a local buckling occurs when the product of the stress and the curvature radius satisfies the following condition (see Eq. (29)):

$$\sigma_{cr}\rho_{cr} = \frac{Eh}{\sqrt{3(1-\nu^2)}} \tag{A.10}$$

Substituting Eqs. (A.8) and (A.9) into Eq. (A.10) yields,

$$\frac{M_{cr}}{M_0} = \frac{\left(1-\frac{3}{2}\xi_{cr}\right)(1-3\xi_{cr})}{(1-\xi_{cr})} \tag{A.11}$$

Since the buckling point is one of the points on the moment versus curvature curve M_{cr}, C_{cr} and ξ_{cr} can be solved from Eqs. (A.1), (A.2) and Eq. (A.11). Substituting Eqs. (A.2) and (A.11) into Eq. (A.1) yields,

$$\sqrt{3\xi_{cr}}(1-\xi_{cr}) = 1-3\xi_{cr} \tag{A.12}$$

from which, we obtain,

$$\xi_{cr} = 0.1453 \tag{A.13}$$

Eq. (A.13) is substituted into Eqs. (A.1) and (A.2), yielding

$$C_{cr} = 0.8085C_b = 0.6601C_0 \tag{A.14}$$

$$M_{cr} = 0.9485M_b = 0.5163M_0 \tag{A.15}$$

This indicates that the critical moment associated with local buckling is about 5% lower than the limit moment given by Brazier. Thus, the local buckling occurs before the limit point is reached.

Appendix B. Derivation of (Eq. 31)

The local radius of circumferential curvature is obtained by calculating the second-order derivative of the deformed cross-section (see Fig. 9(B)) as follows:

$$\rho = -\left(\frac{d^2z}{dy^2}\right)^{-1}\Bigg|_{\theta=0} \tag{B.1}$$

where z and y are the horizontal and vertical coordinates which are defined by

$$y = (R + w_2\cos 2\theta)\sin\theta - \left(\frac{w_2}{2}\sin 2\theta\right)\cos\theta \tag{B.2}$$

$$z = (R + w_2\cos 2\theta)\cos\theta + \left(\frac{w_2}{2}\sin 2\theta\right)\sin\theta \tag{B.3}$$

Substituting Eqs. (B.2) and (B.3) into Eq. (B.1), we have,

$$\rho = \frac{R^2}{R + 3w_2}. \tag{B.4}$$

References

Aksel'rad, E.L., 1965. Pinpointing the upper critical bending load of a pipe by calculating geometric nonlinearity. Izv. Akad. Nauk SSR Mekh. 4, 133–139.

Aksel'rad, E.L., Emmerling, F.A., 1984. Collapse load of elastic tubes under bending. Isr. J. Technol. 22, 89–94.

Brazier, L.G., 1927. On the flexture of thin cylindrical shells and other thin sections. Proc. R. Soc. Ser. A, London, UK 116, 104–114.

Calladine, C.R., 1983. Theory of Shell Structures. Cambridge University Press, Cambridge.

Fabian, O., 1977. Collapse of cylindrical elastic tubes under combined bending, pressure and axial loads. Int. J. Solids Struct. 13, 1257–1270.

Li, L.Y., 1996. Bending instability of composite tubes. J. Aerospace Eng. ASCE 9, 59–61.

Libai, A., Bert, C.W., 1994. A mixed variational principle and its application to the nonlinear bending problem of orthotropic tubes—II. Application to nonlinear bending of circular cylindrical tubes. Int. J. Solids Struct. 31, 1019–1033.

Reissner, E., 1959. On finite bending of pressured tubes. J. Appl. Mech., ASME 26, 386–392.

Seide, P., Weingarten, V.I., 1961. On the buckling of circular cylindrical shells under pure bending. J. Appl. Mech., ASME 28, 112–116.

Stephens, W., Starnes Jr., J.H., Almroth, B.O., 1975. Collapse of long cylindrical shells under combined bending and pressure loads. AIAA J. 13, 20–25.

Tatting, B.F., Gurdal, Z., Vasiliev, V.V., 1995. Nonlinear shell theory solution for the bending response of orthotropic finite length cylinders including the Brazier effect. Proceedings of the 36th Structures, Structural Dynamics and Materials Conference, New Orleans, LA, pp. 966–976.

Tatting, B.F., Gurdal, Z., Vasiliev, V.V., 1997. The Brazier effect for finite length composite cylinders under bending. Int. J. Solids Struct. 34, 1419–1440.

Vasiliev, V.V., 1993. Mechanics of Composite Structures. Taylor and Francis, Washington, DC.